RESULTS OF TESTING THE 3.5M WIYN TELESCOPE PRIMARY MIRROR AND ITS SUPPORT, THERMAL CONTROL, AND ACTIVE OPTICS SYSTEMS

Larry W. Goble
Gary Poczulp
Nicolas Roddier
Larry Stepp

NOAO Preprint No. 447

To be published in: *The Proceedings of the ESO Workshop on Progress in Telescope and Instrumentation Technologies, Garching, April 27-30, 1992*

RESULTS OF TESTING THE 3.5M WIYN TELESCOPE PRIMARY MIRROR AND ITS SUPPORT, THERMAL CONTROL, AND ACTIVE OPTICS SYSTEMS

Larry W. Goble
National Optical Astronomy Observatories*
P.O. Box 26732
Tucson, AZ 85726-6732

Gary Poczulp
National Optical Astronomy Observatories*
P.O. Box 26732
Tucson, AZ 85726-6732

Nicolas Roddier
National Optical Astronomy Observatories*
P.O. Box 26732
Tucson, AZ 85726-6732

Larry Stepp
Gemini 8-M Telescopes Project
P.O. Box 26732
Tucson, AZ 85726-6732

To be published in: *The Proceedings of the ESO Workshop on Progress in Telescope and Instrumentation Technologies, Garching, April 27-30, 1992*

* The National Optical Astronomy Observatories are operated by the Association of Universities for Research in Astronomy, Inc. (AURA) under cooperative agreement with the National Science Foundation.

RESULTS OF TESTING THE 3.5M WIYN TELESCOPE PRIMARY MIRROR AND ITS SUPPORT, THERMAL CONTROL, AND ACTIVE OPTICS SYSTEMS

Larry W Goble, Gary Poczulp, and Nicolas Roddier
National Optical Astronomy Observatories††

P.O. Box 26732, Tucson, Arizona 85726-6732

Larry Stepp
Gemini 8-M Telescopes Project
P.O. Box 26732, Tucson, Arizona 85726-6732

1. INTRODUCTION

Part of the design effort for the Wisconsin-Indiana-Yale-NOAO (WIYN) telescope has been assembly and testing of a prototype primary mirror and cell. In this assembly the mirror, temporarily figured with a spherical surface, is supported on a welded steel cell using a combination of passive hydraulic and active motor-spring mechanisms. Also in the assembly is a mirror temperature regulation system to make the glass uniform in temperature and control the face plate to the surrounding air temperature. The spherical optical surface has allowed evaluation of the overall system performance without the complication of null lens systems. Scatterplate interferometry was used to obtain the optical phase contour maps that are presented. The assembly was mounted on our polishing machine tilt-table, which allowed evaluation of the system in zenith and horizon positions. The test data has been used to evaluate the relation between measured optical surface distortions and several variables, including mirror orientation (vertical or horizontal), temperature, dynamic temperature environment, thermal regulation on or off, and active support force changes. In addition, valuable information was learned about the vibration effects caused by active components on the mirror cell, the correction of residual thermal bending through the use of active forces, and the functionality of the parts used to make the assembly. Software required to control the active systems was developed and tested on the prototype system.

2. HARDWARE SYSTEMS

The 2000 Kg primary mirror is a borosilicate honeycomb casting which was the second of its size cast at the University of Arizona. The mirror is supported on a hollow core welded steel structure using a passive whiffletree support system.

In the axial direction, 66 support points are arranged in three zones. In the lateral direction, support is applied at 24 points at selected holes in the back-plate. Each support point has a hydraulic piston that is connected to the other points in the same zone with a tubing manifold. Pressure from the lateral support is coupled to the axial system using another set of pistons designed to compensate for the bending effects caused

††Operated by the Association of Universities for Research in Astronomy, Inc. under cooperative agreement with the National Science Foundation.

by supporting at the back of the mirror. Passive support pressures are 171 Kpa in the lateral system and 70.3 Kpa in the axial system. The stiffness of the two directions are 47000 N/mm lateral and 610000 N/mm axial.

Active force control is incorporated into the mechanisms at the 66 axial supports. Stepper motors drive lead screws through gearboxes. The screws deflect springs that are connected to the support points. Forces of +/- 1100 N can be applied with accuracy of one newton.

The position of the mirror relative to the cell is determined by LVDT measurements at four places. Three are at the centroids of the axial support zones, and one measures parallel to the lateral support. The dimension at the LVDT's is adjusted by adding ,or subtracting, fluid to each passive support zone. The cross-lateral and twisting directions are constrained by rigid arms.

The temperature of the mirror is regulated using thermally controlled air distributed through the enclosed steel box support cell and forced through 354 nozzles into the mirror structure. Motion of the air is forced by 12 squirrel-cage blowers that act in parallel through 12 fin-tube heat exchangers. The air circulating behind the mirror is a closed system. Thermal control is accomplished by setting the temperature of the liquid coolant flowing into the 12 heat exchangers. When the coolant flows away from the mirror cell the heat is taken with it.

3. TESTING GOALS

Goals for our test program can be divided into two categories. First, we wanted to test the actual prototype systems to be used in the telescope; and second, we needed to answer some questions about general design strategies for using borosilicate honeycomb mirrors. We had in mind the following procedures to accomplish these goals.

- Run optical tests with the mirror pointing in the vertical and horizontal directions. Our horizontal tests were done at vertical minus 82 degrees. The method allows evaluation of the effects of transfer of the mirror weight from the axial supports to the lateral.
- Make corrections to the optical surface with the 66 axial active supports.
- Run tests to calibrate the influence of each active support on the optical surface.
- Look at motion of the image while running the subsystems. Of interest are the motion while changing the active supports, while running the on-cell blowers, and while running the thermal control fluid pump.
- Make direct comparisons of optical test data from the mirror surface instead of measuring other parameters and linking the results to optical performance with analysis.
- Run the system for long time periods to identify system problems that should be corrected before installation on the mountain.

A large number of questions have been answered by these tests, but there is not space to discuss all of the results. A subset of these are listed below, and the answers are addressed in subsequent sections.

- On the passive support, how much will the figure change between zenith and horizon?
- Will adjustments of the active support forces produce unacceptable image motion?
- Will the thermal regulation system maintain sufficient control in a changing environment such as will be present on a mountaintop?

- Can the active support system correct the residual distortion not controlled by the thermal control system, or will uncorrectable high-spatial-frequency surface errors occur?
- Can the active optics system correct all thermal distortions, eliminating the need for a thermal regulation system?
- Will the on-board blowers produce unacceptable image motion?

4. DISCUSSION OF SELECTED RESULTS

Selected test results are presented in figures 1-7. In each figure, the peak-to-valley variations (P/V) and root-mean-square variations (RMS) are shown near the top of the map. For the optical surface maps the values are in wavelengths, at the testing wavelength of 632.8 nm. For the thermal maps the values are in degrees C.

In figure 1 the left and right contour maps show the mirror surface accuracy at zenith and horizon, respectively, after active optics optimization. The center map shows the zenith-to-horizon change in the figure of the mirror that occurred on the passive support, before making the active optics correction.

Some of the active optics exercises performed on the mirror created the maps displayed in figures 2 and 3. In each case, the contour map in figure 2 is the actual change in mirror figure, while the contour map directly below in figure 3 shows the intended change.

Figures 4, 5 and 6 are thermal maps, with temperature variations displayed in a continuous gray-shade scale. In each figure, the left map shows the temperature of the front faceplate of the mirror, the center map shows the air temperatures in the honeycomb core, and the right map shows the temperature of the backplate. Each of these is based on temperatures measured by 294 evenly-distributed thermal sensors. The upper rectangle below the three circular maps depicts temperatures measured at the mid-level of the inside diameter of the mirror, with the left end of the rectangle corresponding to the 12 o'clock position of the circular map. The lower rectangle shows the corresponding temperatures around the outside diameter. Units are degrees Celsius. To minimize the effect of zero-point calibration errors, a reference thermal map has been subtracted from the data in figures 4 5 and 6. This reference condition was measured under stable laboratory conditions. We estimate the systematic temperature profile removed from the data by this subtraction is less than 0.03 degrees RMS. Note that when the thermal regulation system is operating the measured mean value of the backplate is essentially the same as the measured mean value of the faceplate. A difference to the mean value measured for the internal air means that there is some heat transfer taking place.

In figure 6, the thermal map shows the difference between two data sets measured after and before the blower speeds were adjusted to equalize the exit air temperatures at the heat exchangers. Figure 7 shows the corresponding change in the mirror surface. The close comparison between the two gives us confidence that the resolution and repeatability of both the optical testing and the thermal measurement are excellent. Also, our calculations show that the surface distortions resulted almost entirely from rib growth. rather than from bending effects. This implies that in our system changes in blower speed do not result in front-to-back thermal gradients. Past experiments at NOAO have shown bending effects tend to dominate the thermal distortions of borosilicate mirrors without thermal regulation systems.

In this and the following four paragraphs, we discuss the answers to the questions raised in section 3. Figure 1 answers the question about the change in mirror figure between zenith and horizon. The relatively small support errors in the passive system confirm our previous analysis conclusions about the feasibility of lateral support from the backplate. However, the existence of these errors, and the ability to completely eliminate them, highlight the advantage of incorporating the active optics supports into the design.

Tests made with an autocollimating microscope at the center of curvature of the mirror indicate that image motion is less than 0.05 arc second when large active optics adjustments are made with this system.

Tests that exposed the mirror system to a dynamically changing thermal environment show unacceptable distortions can result, that are mostly astigmatism. Astigmatism is effectively corrected with the active optics system.

When the thermal control system is not running, the edge of the mirror can easily change temperature, even in the optics shop, in ways that cannot be corrected by the active optics system.

Additional tests made with the autocollimating microscope show that the on-board blowers do not produce detectable image motion (0.05 arc second or greater) when running steadily; however, they do produce momentary vibrations resulting in about 0.10 arc second of image motion when first ramping up to their running speed.

5. CONCLUSIONS

The information learned from these tests has not only been a step forward in designing the WIYN primary mirror system, it has also provided important information for upcoming telescope projects that are considering use of the borosilicate mirrors. The overall performance of the prototype design is good and we believe that the basic design allows full compliance with requirements. However, some areas of the hardware have been identified for improvement.

The active optics system does a good job of correcting low order optical surface aberrations. However, a comparison of figures 2 and 3 shows that, because of the mirror's high structural bending stiffness, attempts to correct spherical aberration result in a hexagonally distorted shape similar to the mirror rib geometry, with print-through bumps showing where the loads are applied. Radial-direction bending of the mirror near the outer edge is not effective because no supports are placed at the extreme edge. Correction of trefoil is much better because the bending at the edge is tangential. This has implications for the design of the thermal control system. Our system is designed with control areas arranged in sectors. Note the pattern of temperature in figure 6. This error shape can be better corrected by the active optics system than other shapes.

Our tests have demonstrated that both a thermal control system and an active optics system are needed for our borosilicate honeycomb mirror system. However, with both systems in place, the performance of these mirrors is excellent.

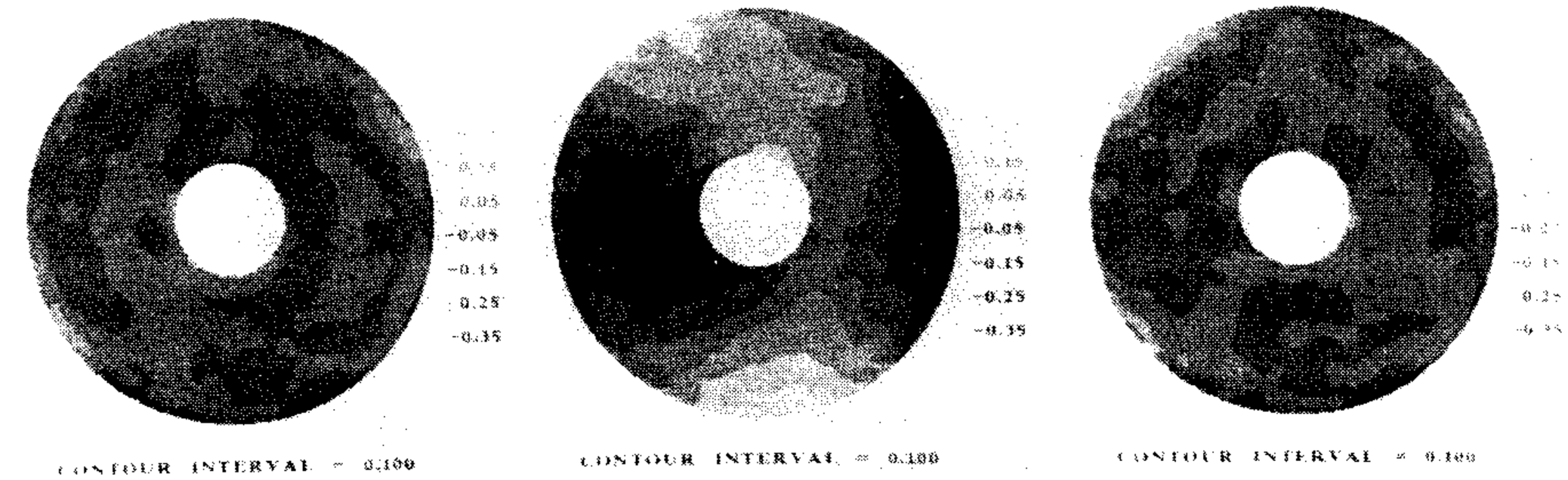

Figure 1. The left display shows the optical surface accuracy while zenith pointing, the center shows the change due to tilting 82 degrees toward the horizon, and the right display shows the horizon pointing surface accuracy after active optics corrections.

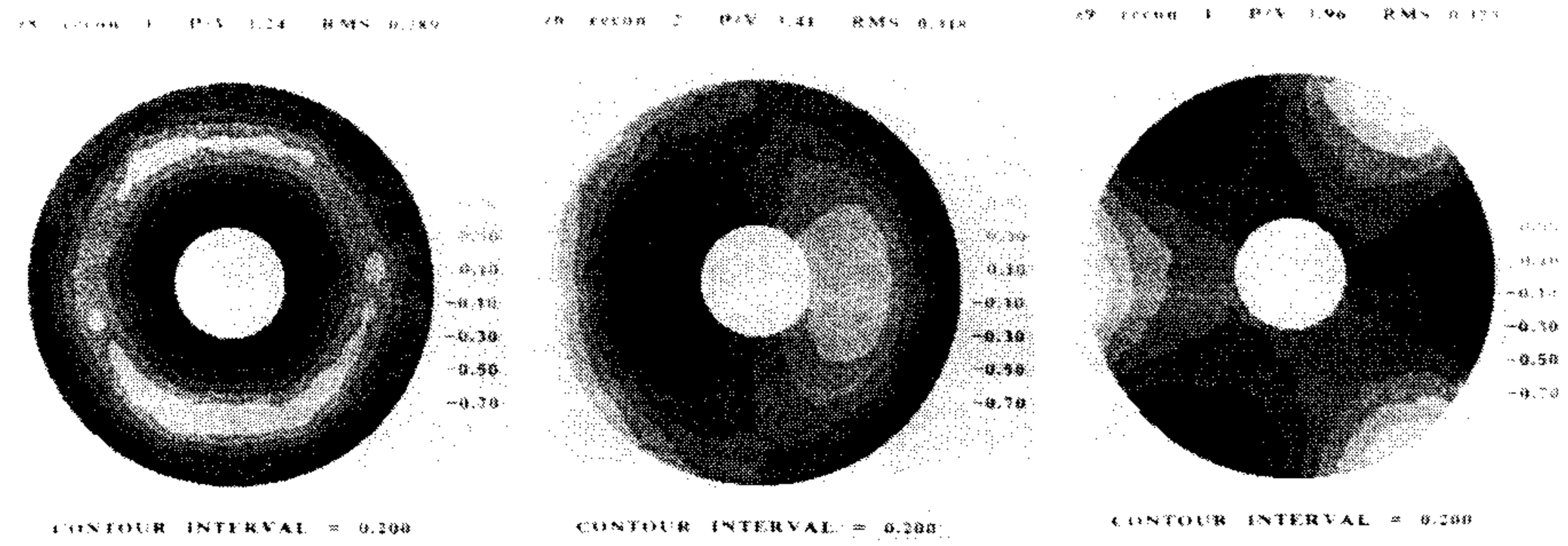

Figure 2. These are low order Zernike shapes that we created using the 66 active axial supports. They can be compared with the goals shown in the next figure. The left display corresponds to spherical aberration. the center corresponds to coma, and the right is trefoil.

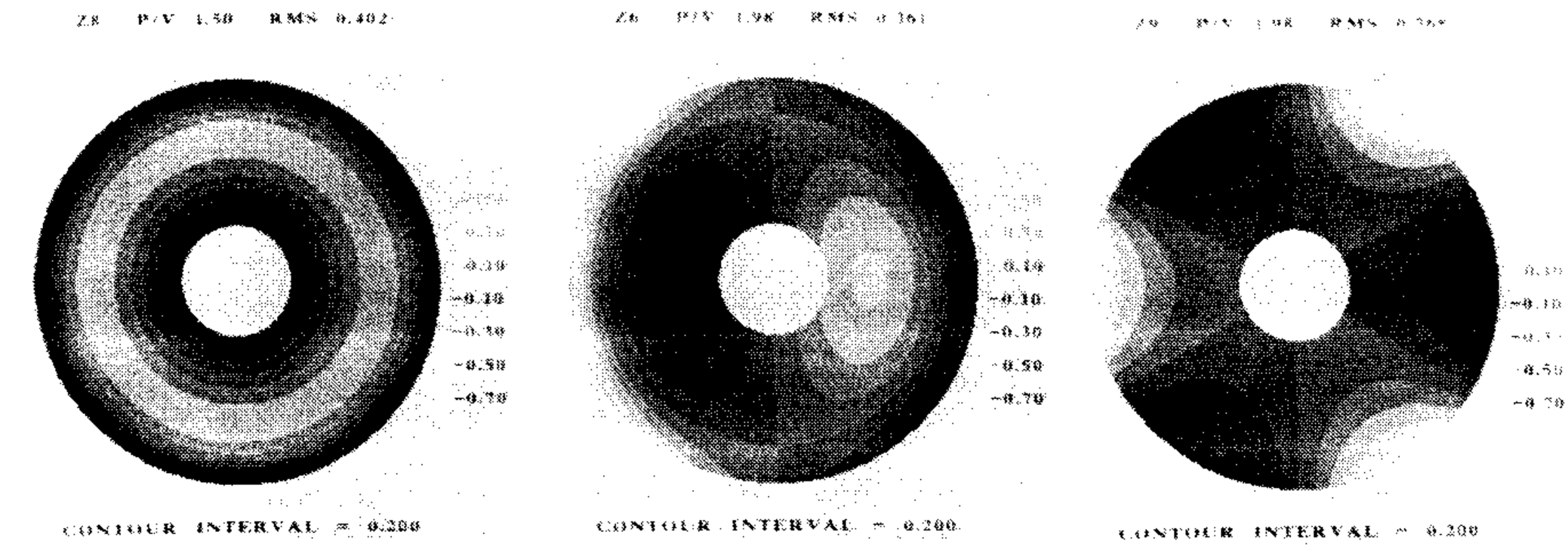

Figure 3. The mathematical functions that served as goals for the surfaces shown in figure 2.

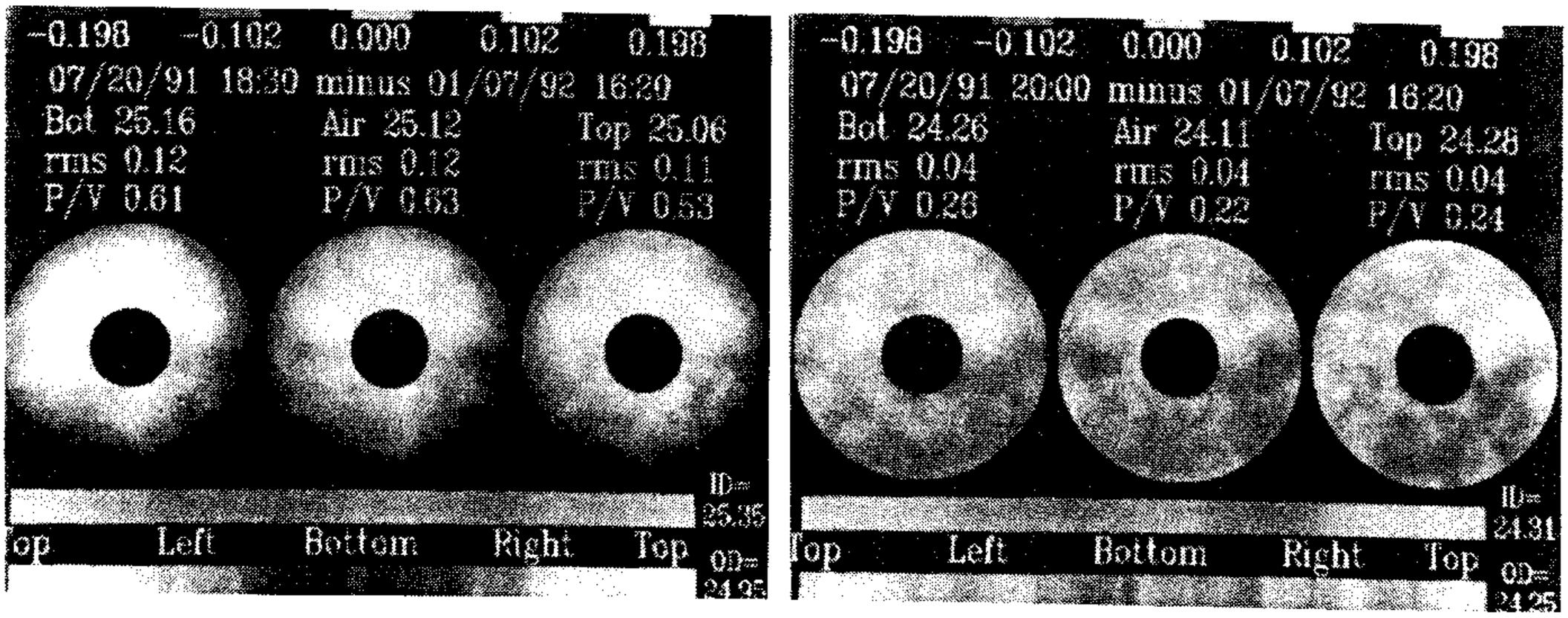

Figure 4. Temperature variations in the mirror early in the test program. The left set is without thermal control and the right is after running the thermal control system for 1.5 hours.

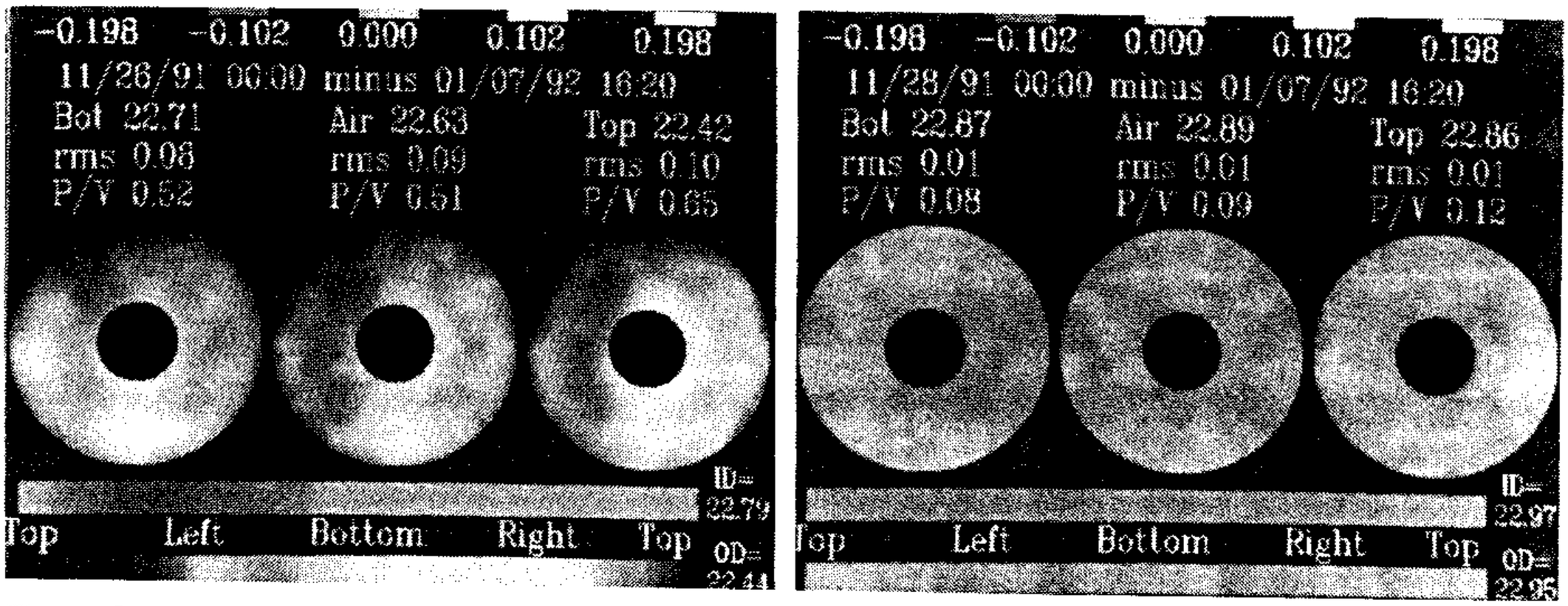

Figure 5. Temperature variations after some improvements on the thermal control system. The left map is the result of another time when the thermal control system was off. The right map was taken two days later when the system was running in the steady state.

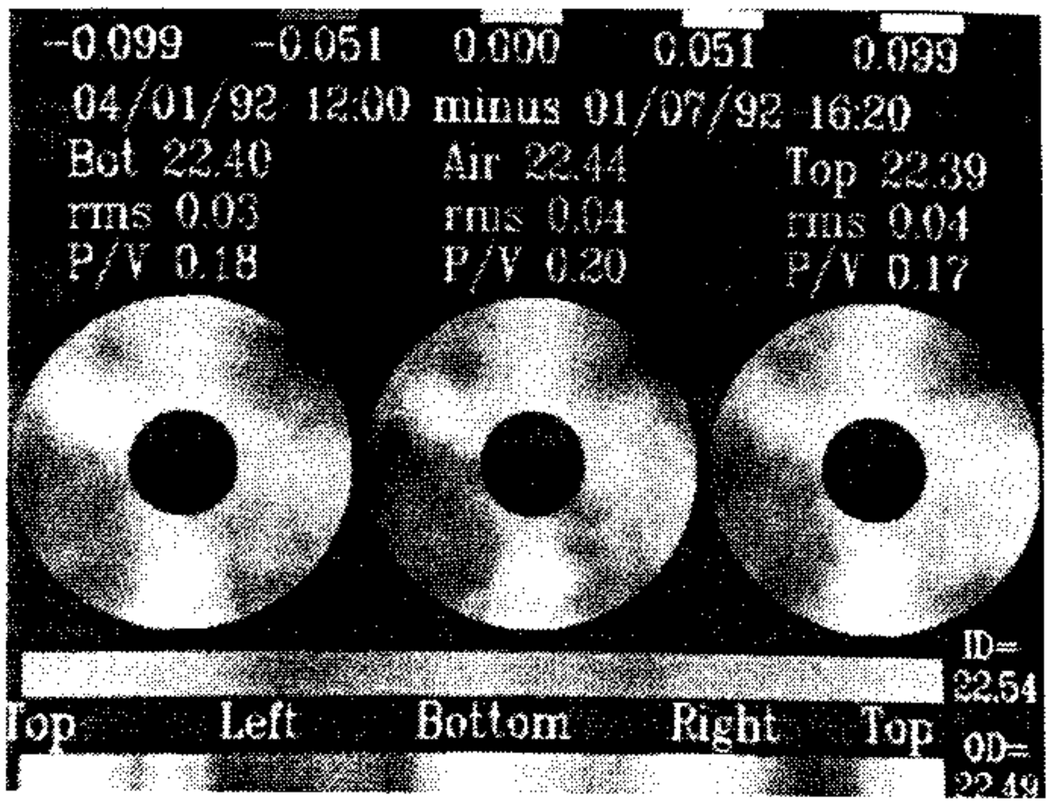

Figure 6. Temperature changes resulting from relatively large adjustments on the 12 blowers to make the exit temperatures from the heat exchangers match.

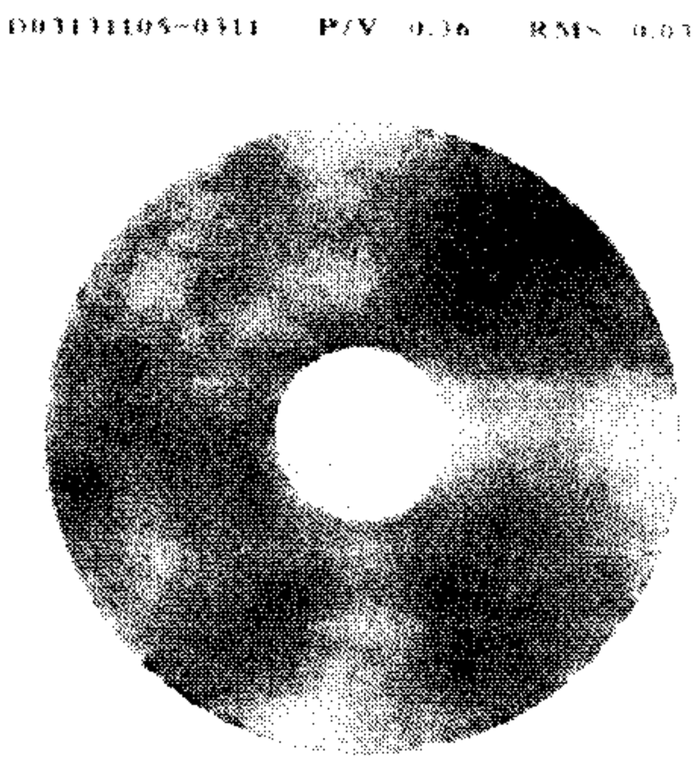

Figure 7. Changes in the mirror surface resulting from the temperature changes in figure 6.